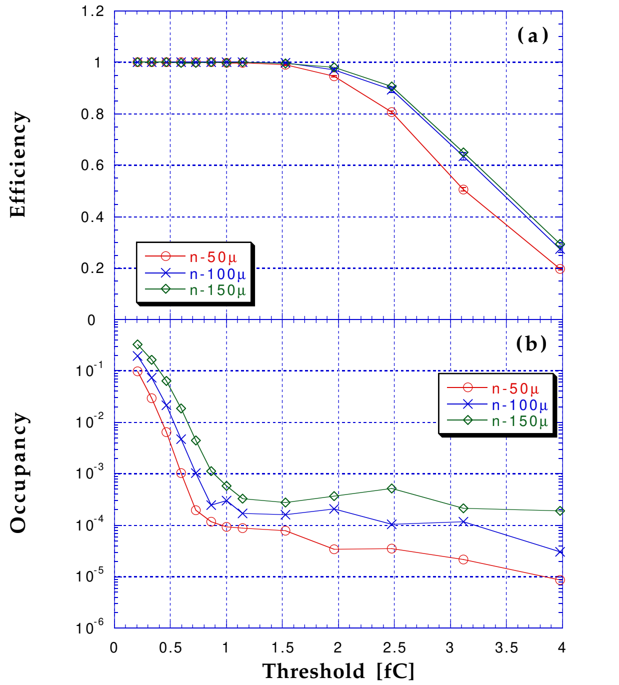

Fig. 5 (a) Efficiency and (b) occupancy as a function of threshold for the normal incident pions. The data were collected for the n-side of the irradiated LBIC-DUT at y=4.2cm and at a bias voltage of 120V. Responses of three pitches are shown: 50µ (circle), 100µ (cross), and 150µ (diamond).

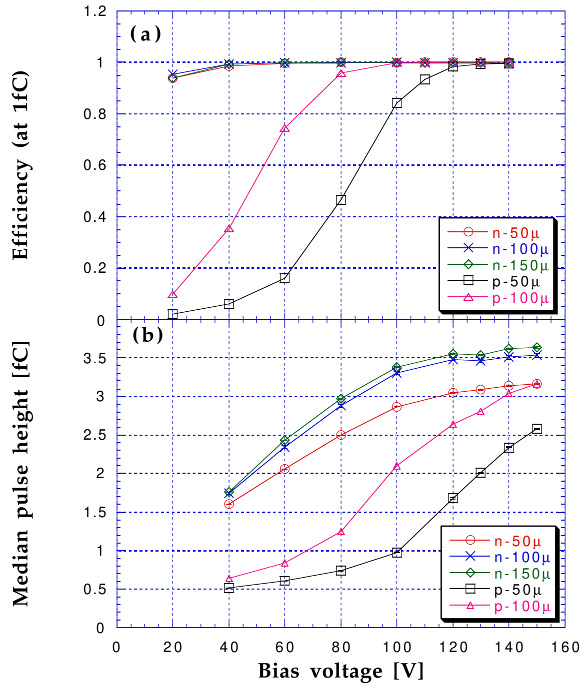

Fig. 7 (a) Efficiency at a threshold of 1fC and (b) the median pulse height distribution as a function of bias voltage for the normal incident pions. The data was collected for the irradiated LBIC-DUT at y=4.2cm: 50µ (circle), 100µ (cross), 150µ (diamond) in the n-side; 50µ (square) and 100µ (triangle) in the p-side.

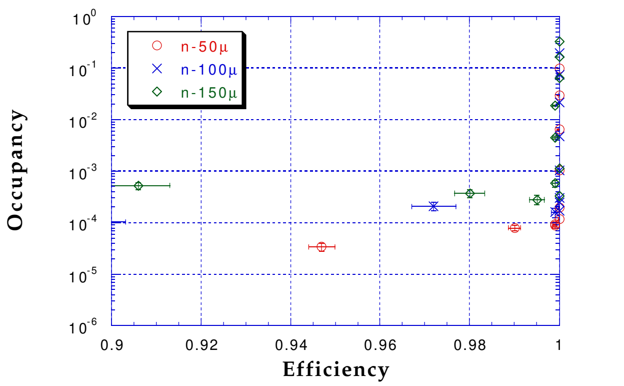

Fig. 6 Efficiency vs. noise occupancy in the irradiated LBIC-DUT at y=4.2cm and at a bias voltage of 120V in the n-side: 50µ (circle), 100µ (cross), 150µ (diamond).

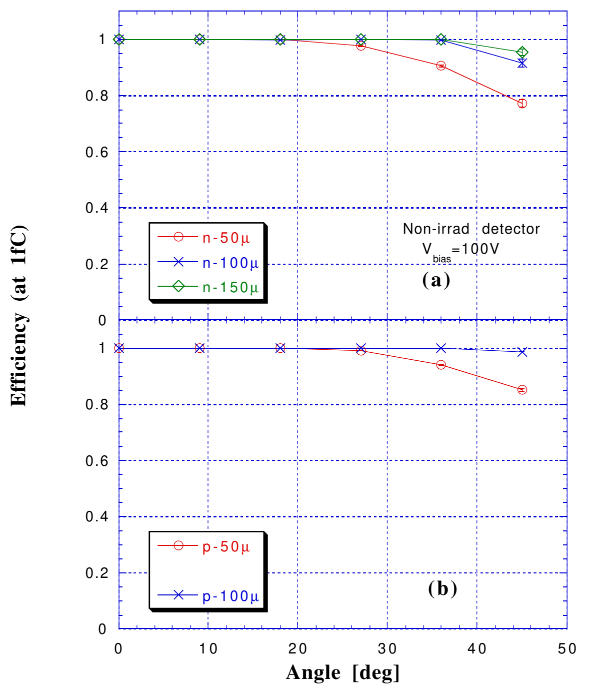

Fig. 8 Angular dependence of the efficiency at the threshold of 1fC for the non-irradiated LBIC-DUT at a bias voltage of 100V: (a) in the n-side: 50µ (circle), 100µ (cross), 150µ (diamond) pitches; (b) in the p-side: 50µ (circle), 100µ (cross) pitches.

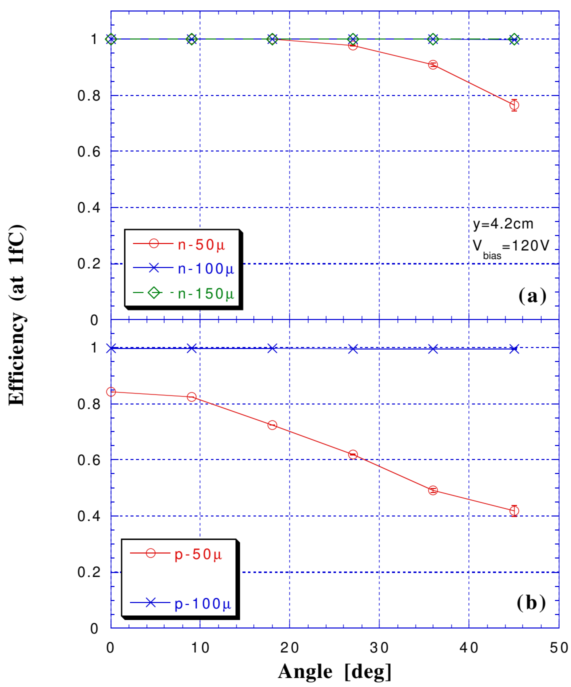

Fig. 9 Angular dependence of the efficiency at the threshold of 1fC for the irradiated LBIC-DUT at a bias voltage of 120V at y=4.2cm: (a) in the n-side: 50µ (circle), 100µ (cross), 150µ (diamond) pitches; (b) in the p-side: 50µ (circle), 100µ (cross) pitches.

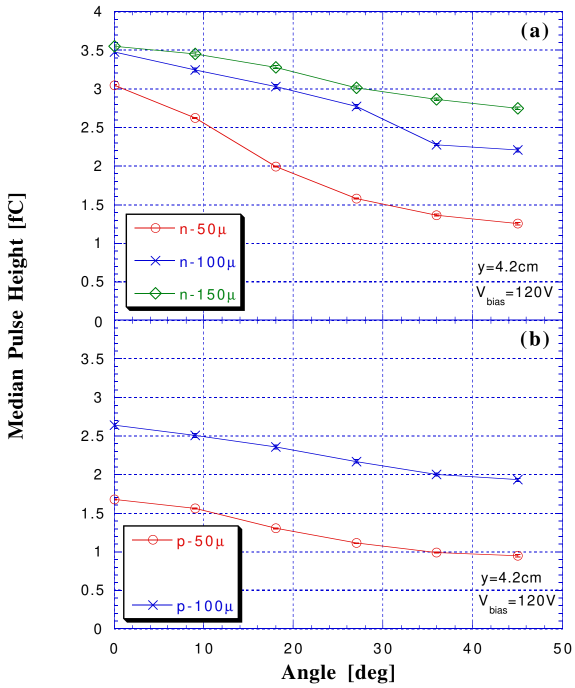

Fig. 10 Angular dependence of the median pulse height of the irradiated LBIC-DUT at the bias voltage of 120V at y=4.2cm: (a) in the n-side: 50µ (circle), 100µ (cross), 150µ (diamond) pitches; (b) in the p-side: 50µ (circle), 100µ (cross) pitches.

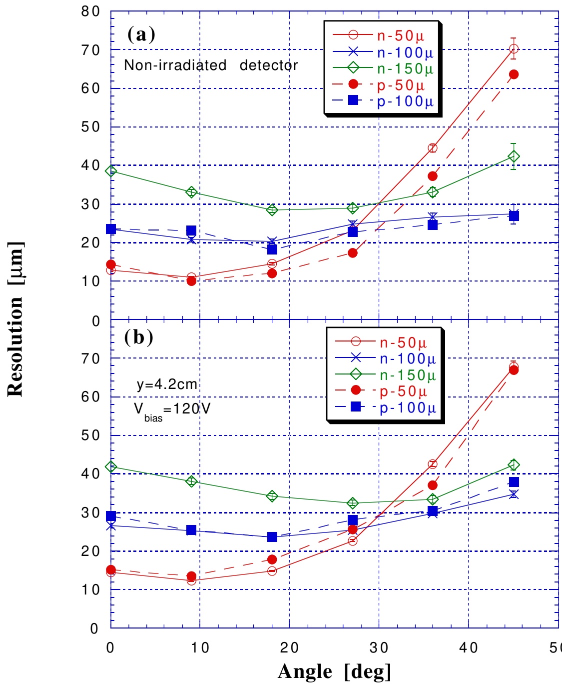

Fig. 11 Spatial resolutions at the threshold of 1fC: (a) the non-irradiated LBIC-DUT at a bias voltage of 100V, 50µ (circle), 100µ (cross), 150µ (diamond) pitches in the n-side, 50µ (filled circle), 100µ (filled square) in the p-side; and (b) the irradiated LBIC-DUT at a bias voltage of 120V and at y=4.2cm, the same designations for the pitches and the marks.

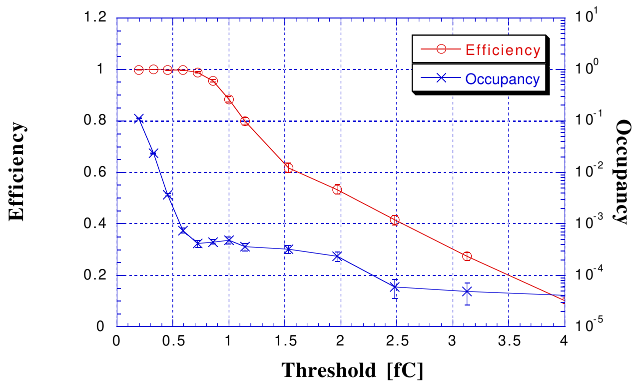

Fig. 13 Efficiency(circle) and noise occupancy(cross) distributions of the 100*µ case in the n-side of the irradiated detector as a function of the threshold at y=4.2cm and at a bias voltage of 120V for the normal incident pions.

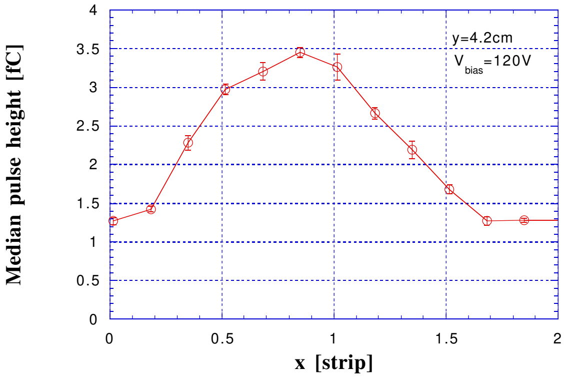

Fig. 14 Local median pulse height distribution in one pitch of the 100*µ case in the n-side of the irradiated detector at y=4.2cm at a bias voltage of 120V for the normal incident pions.

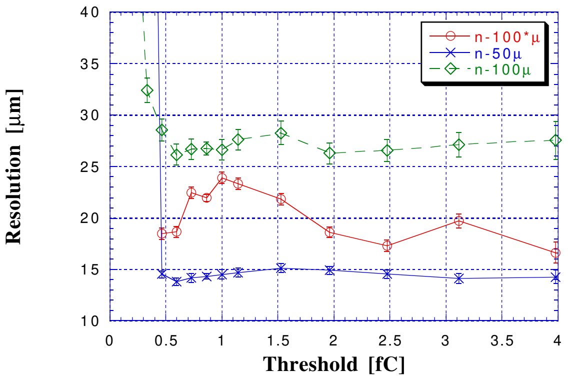

Fig. 15 Spatial resolutions as a function of threshold of the floating-intermediate-readout 100*µ case(circle), the no-intermediate 50µ(cross), and the 100µ (diamond) in the n-side of the irradiated detector at y=4.2cm and at 120V for the normal incident pions.

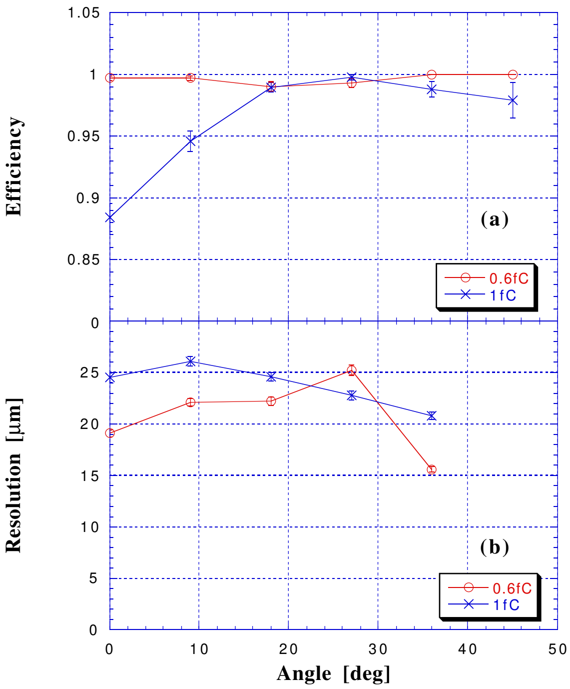

Fig. 16 (a) Efficiencies and (b) spatial resolutions as a function of incident angles for two thresholds: 0.6 fC(circle) and 1.0 fC(cross), in the 100*µ configuration.

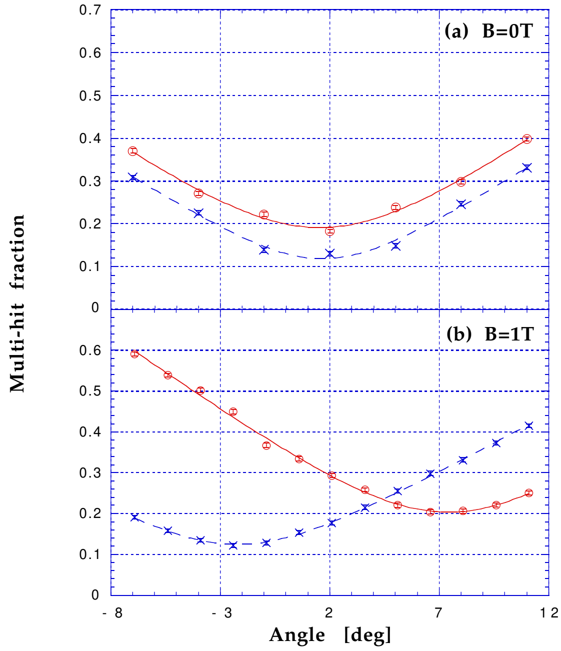

Fig. 18 Multi-strip hit fraction as a function of the ϕ-angles: (a) B=0T, (b) B=1T; n-side (circle/solid line), p-side (cross/dashed line). The minimum was obtained by fitting a hyperbolic function to the data (overlaid curves).